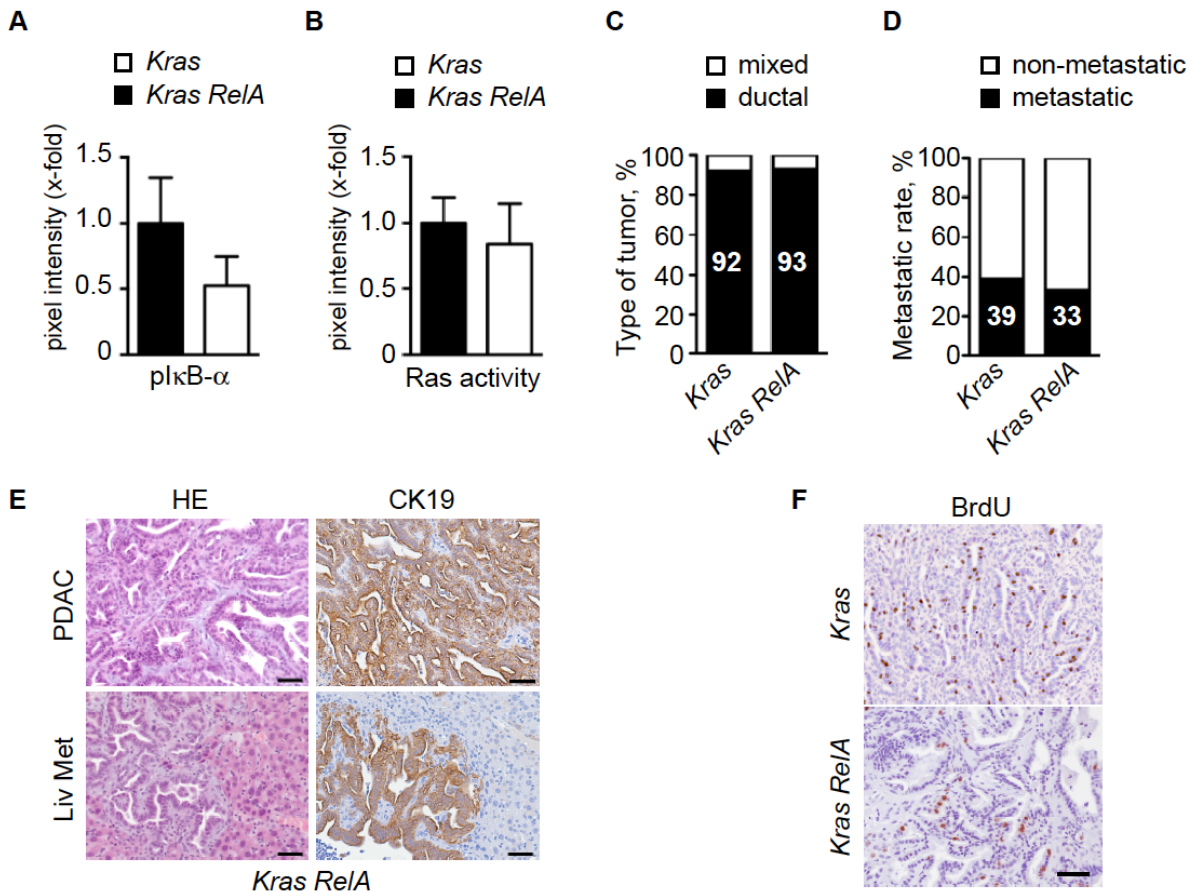


## Supplemental Information

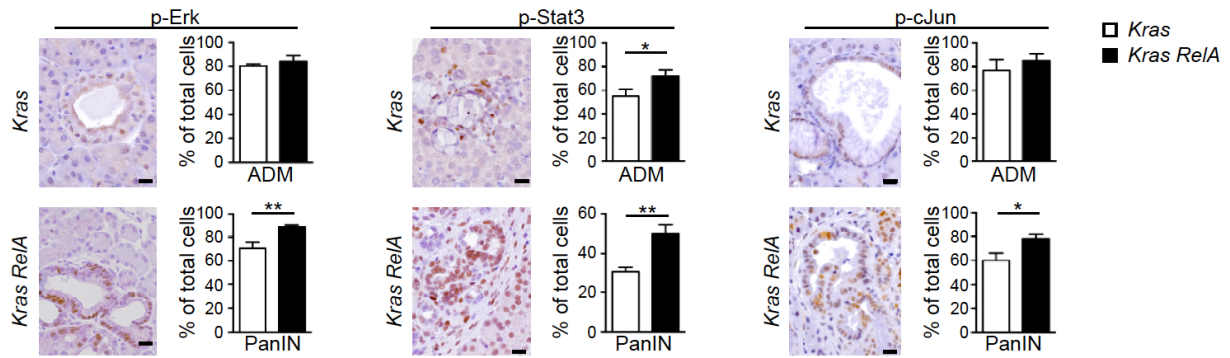
### **RelA regulates CXCL1/CXCR2-dependent oncogene-induced senescence in murine *Kras*-driven pancreatic carcinogenesis**

Marina Lesina<sup>1</sup>, Sonja Maria Wörmann<sup>1</sup>, Jennifer Morton<sup>2</sup>, Kalliope Nina Diakopoulos<sup>1</sup>, Olga Korneeva<sup>1</sup>, Margit Wimmer<sup>1</sup>, Henrik Einwächter<sup>1</sup>, Jan Sperveslage<sup>3</sup>, Ihsan Ekin Demir<sup>4</sup>, Timo Kehl<sup>5</sup>, Dieter Saur<sup>1</sup>, Bence Sipos<sup>6</sup>, Mathias Heikenwälder<sup>7,8</sup>, Jörg Manfred Steiner<sup>1,9</sup>, Timothy Cragin Wang<sup>10</sup>, Owen J. Sansom<sup>2</sup>, Roland Michael Schmid<sup>1</sup>, and Hana Algül<sup>1,11</sup>



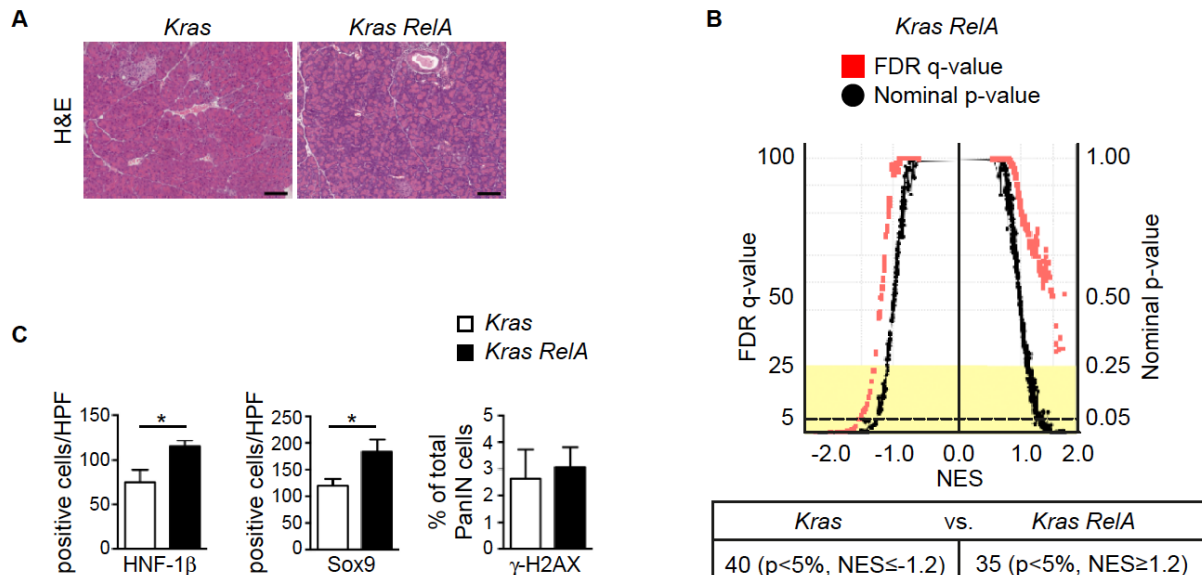
### Supplemental Figure 1. Role of RelA during pancreatic cancer development

(A) Quantification of immunoblot analysis of I $\kappa$ B- $\alpha$  in lysates from 4-week-old *Kras* and *Kras RelA* mice, representing the pixel intensity. Mean  $\pm$  SD. (B) Quantitative analysis of Ras activity in *Kras* and *Kras RelA* mice, representing the pixel intensity. Mean  $\pm$  SD. (C-D) PDAC development in *Kras* and *Kras RelA* mice was monitored by assessing the tumor type (C) and the metastatic rate (D). (E) Representative H&E staining and expression of CK19 (cytokeratin19) in PDAC and liver metastases from *Kras RelA* mice. Positive immunostaining for CK19 was used to confirm the ductal phenotype of liver metastases. Scale bars, 50  $\mu$ m. (F) Representative BrdU staining of PDAC samples from *Kras* and *Kras RelA* mice. Scale bars, 50  $\mu$ m. (G) Western Blot analysis of RelA expression in pancreatic cancer cell lines and in a liver metastatic (LM) cell line isolated from *Kras* and *Kras RelA* mice;  $\beta$ -actin served as loading control. (H) Growth analysis of tumor-derived cell from *Kras* and *Kras RelA* mice. Viable cells were counted at the indicated time points in three independent experiments. Results are presented as Mean  $\pm$  SEM; \*\*\* $p$ <0.0005 by unpaired t test.



**Supplemental Figure 2. Pathways, which are relevant for mPanIN progression were up-regulated in *Kras ReIA* pancreatic tissue**

Representative immunostaining for p-Erk, p-Stat3, p-cJun and quantification of positivity in ADM and PanIN cells in *Kras* (n=3) and *Kras ReIA* (n=3) pancreata. Results are presented as Mean  $\pm$  SD; \*p<0.05, \*\*p<0.005 by unpaired t test; scale bars, 20  $\mu$ m; n: number of mice.



### Supplemental Figure 3. Transcriptomic analysis of *Kras* and *Kras RelA* pancreata

(A) H&E staining of representative samples of pancreatic tissue from *Kras* and *Kras RelA* mice (< 4 weeks of age). Scale bars, 100  $\mu$ m. (B) Normalized enrichment score (NES) vs. significance (nominal p-values, black circles, and false discovery rate [FDR] q-values, red quadrants) plot illustrating transcription factor gene sets enriched in *Kras* (n=4) and *Kras RelA* (n=2) pancreata; gene sets were identified by gene set enrichment analysis (GSEA) software using 579 transcription factor gene sets. Among these gene sets 35 were significantly up-regulated in pancreata from *Kras RelA* mice compared to *Kras* mice (nominal p-value < 0.05, NES  $\geq$  1.2). 40 gene sets, in turn, were upregulated in *Kras* mice compared to *Kras RelA* pancreata (nominal p-value < 0.05, NES  $\leq$  -1.2); the enriched gene sets are localized below the dotted line in the diagram. (C) Quantification of HNF-1 $\beta$ , Sox9, and  $\gamma$ -H2AX positivity in *Kras* (n=3) and *Kras RelA* (n=3) mice. Mean  $\pm$  SD; \*p < 0.05, by unpaired t test; 200x optical field (high power field, HPF); n: number of mice.

**Supplemental Table 1. Comparison of the classification of up-regulated gene sets in histopathologically normal pancreata from *Pdx1-cre;Kras<sup>LSL-G12D</sup>;IKK2/ $\beta$ <sup>F/F</sup>* and *Pdx1-cre;Kras<sup>LSL-G12D</sup>* mice and *Kras RelA* and *Kras* mice (p<0.01) (1)**

**A KEGG Signatures**

<b><i>Pdx1-cre;Kras<sup>LSL-G12D</sup>;IKK2/<math>\beta</math><sup>F/F</sup></i> versus <i>Pdx1-cre;Kras<sup>LSL-G12D</sup></i></b>		
Gene Name	NES	NOM p-val
KEGG_OXIDATIVE_PHOSPHORYLATION	2,39	0
KEGG_PARKINSONS_DISEASE	2,16	0
KEGG_CITRATE_CYCLE_TCA_CYCLE	2,07	0
KEGG_HUNTINGTONS_DISEASE	2,05	0
KEGG_ALZHEIMERS_DISEASE	2,00	0
KEGG_PROPANOATE_METABOLISM	1,99	0
KEGG_VALINE_LEUCINE_AND_Isoleucine_DEGRADATION	1,91	0
KEGG_PYRUVATE_METABOLISM	1,89	0.0015
KEGG_PYRIMIDINE_METABOLISM	1.75	0
KEGG_GLYCOLYSIS_GLUconeogenesis	1.62	0.0082
KEGG_RIBOSOME	2.39	0
KEGG_PROTEIN_EXPORT	2.18	0
KEGG_AMINOACYL_TRNA_BIOSYNTHESIS	1.77	0.0044
KEGG_RNA_POLYMERASE	1.76	0.0029
KEGG_SPLICEOSOME	1.71	0
KEGG_BIOSYNTHESIS_OF_UNSATURATED_FATTY_ACIDS	1.67	0.0079
KEGG_PROTEASOME	2.16	0
KEGG_UBIQUITIN_MEDIATED_PROTEOLYSIS	1.56	0.0036
KEGG_CELL_CYCLE	1.75	0
KEGG_DNA_REPLICATION	1.64	0.0058

<b><i>Kras RelA</i> versus <i>Kras</i></b>		
Gene Name	NES	NOM p-val
KEGG_DRUG_METABOLISM	1.75	0.0038
KEGG_CYTOCHROME_P450		
KEGG_MATURITY_ONSET_DIABETES_OF_THE_YOUNG	1.87	0

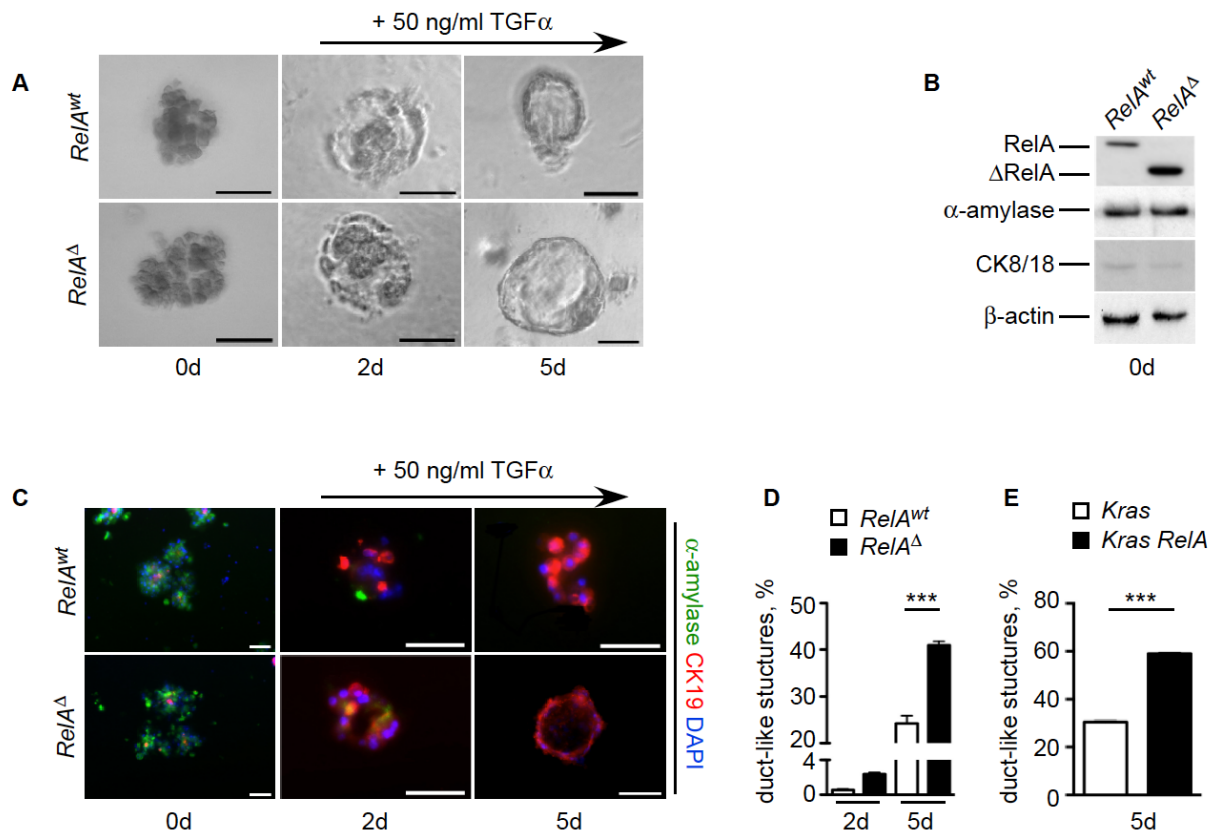
METABOLISM
BIOSYNTHESIS
CELL STRESS
CELL CYCLE
CELL DIFFERENTIATION

B Transcription Factor Signatures

<b><i>Pdx1-cre;Kras<sup>LSL-G12D</sup>;IKK2/<math>\beta</math><sup>F/F</sup></i></b> <b>versus <i>Pdx1-cre;Kras<sup>LSL-G12D</sup></i></b>		
Gene Name	NES	NOM p-val
V\$ELK1_02	1.97	0
V\$MAX_01	1.81	0
V\$MYC_Q2	1.79	0
V\$MYCMAX_01	1.77	0
V\$MYCMAX_B	1.70	0
V\$NMYC_01	1.55	0
V\$MYCMAX_03	1.50	0.0046
V\$CREB_02	1.41	0.0078
V\$ARNT_01	1.87	0
V\$NRF1_Q6	1.79	0
V\$NRF2_01	1.71	0
TTGCWCAAY_V\$CEBPB_02	1.52	0.0095
V\$ARNT_02	1.50	0
V\$XBP1_01	1.50	0.0073
V\$GABP_B	1.49	0
V\$HIF1_Q3	1.45	0.0035
TGANNYRGCA_V\$TCF11MAFG_01	1.45	0.0023
V\$YY1_02	1.44	0.0023
V\$YY1_Q6	1.43	0.0023
V\$TGIF_01	1.41	0.0092
GCCATNTTG_V\$YY1_Q6	1.40	0.0021
V\$E2F1_Q6	1.76	0
SGCGSSAAA_V\$E2F1DP2_01	1.75	0
V\$E2F_02	1.74	0
V\$E2F4DP2_01	1.71	0
V\$E2F_Q3	1.71	0
V\$E2F1DP2_01	1.71	0
V\$E2F4DP1_01	1.69	0
V\$E2F1DP1_01	1.69	0
V\$E2F1_Q3	1.65	0
V\$E2F_Q2	1.65	0.0012
V\$CETS1P54_01	1.64	0
V\$E2F_Q4	1.62	0
V\$E2F1_Q3_01	1.60	0
V\$E2F_Q6	1.58	0
V\$E2F_Q4_01	1.58	0
V\$E2F_Q3	1.58	0
V\$E2F1_Q6_01	1.56	0.0023
V\$E2F1DP1RB_01	1.55	0.0012
V\$E4F1_Q6	1.52	0
V\$E2F_Q3_01	1.49	0.0035
V\$TEL2_Q6	1.47	0.0034
V\$E2F_Q6_01	1.41	0.0080
V\$E2F1_Q4_01	1.50	0.0023
V\$ELK1_01	1.40	0.0034

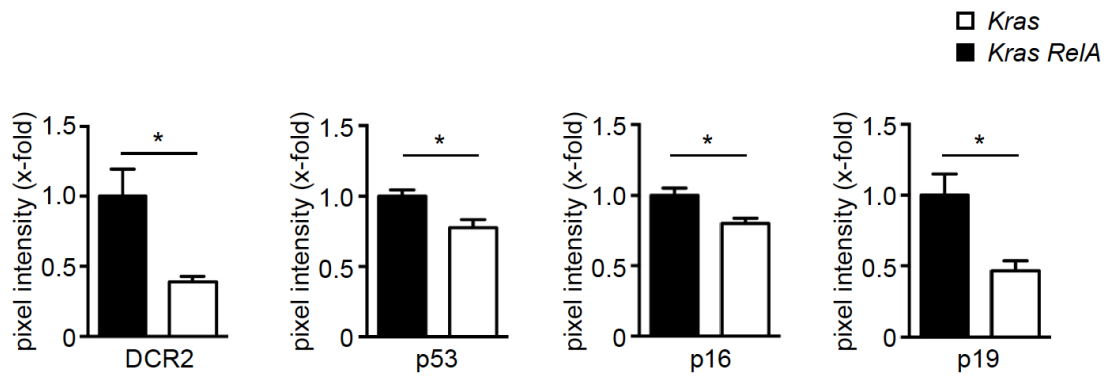
<b><i>Kras RelA versus Kras</i></b>		
Gene Name	NES	NOM p-val
V\$OCT1_02	1.54	0.0035
V\$SOX9_B1	1.48	0.0034
V\$OCT1_06	1.29	0.0535

MYC/SREBP/CREB
NRF/HIF/CELL STRESS
E2F/ETS
INFLAMMATION
CELL DIFFERENTIATION



#### Supplemental Figure 4. Analysis of RelA involvement in ADM

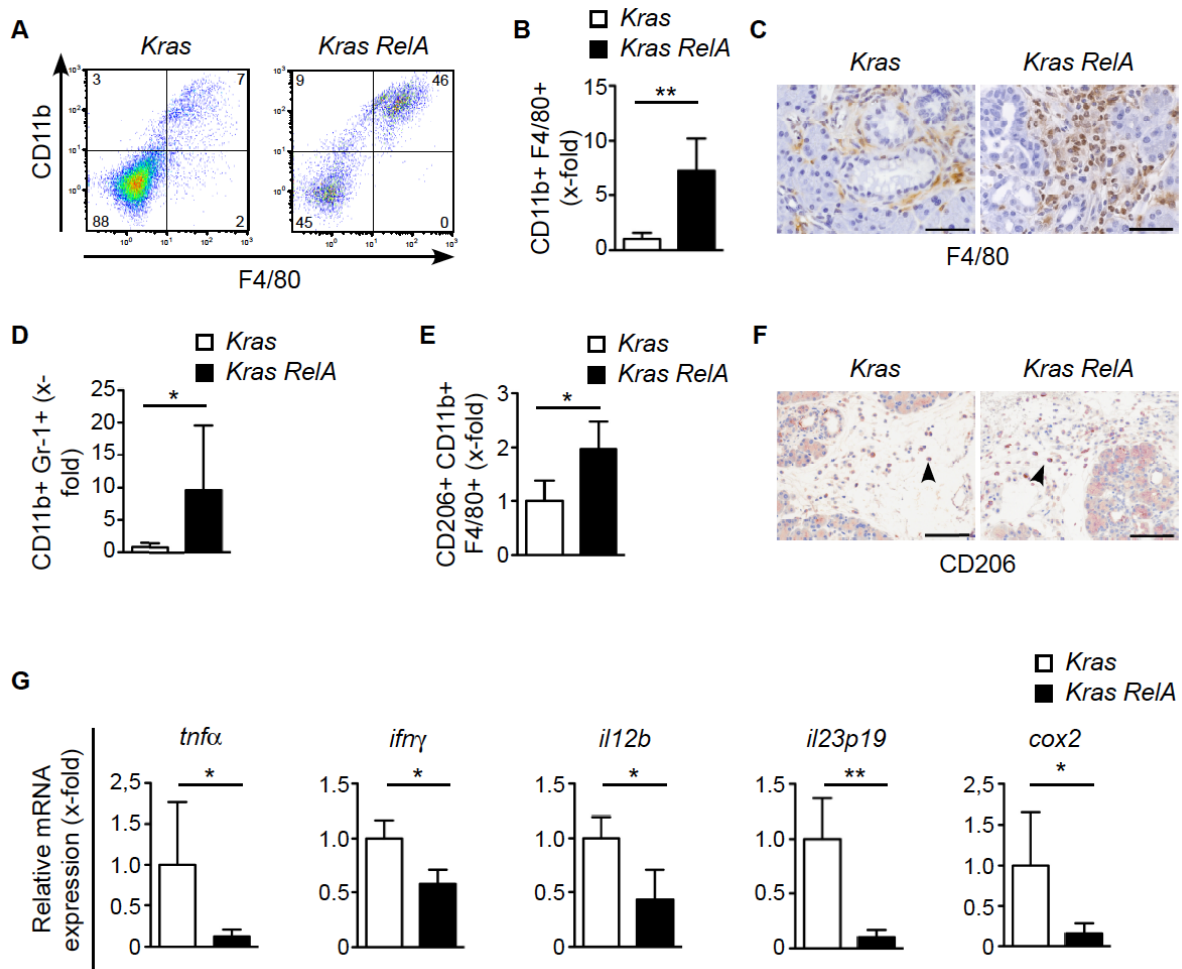
(A) Phase contrast images of acinar explants from *RelA*<sup>wt</sup> and *RelA*<sup>Δ</sup> pancreata, which convert to duct-like structures when cultured with 50ng/ml TGF $\alpha$  for 0, 2, and 5 days. Scale bars, 50  $\mu$ m. (B) Western Blot analysis of lysates from freshly isolated acinar explants from *RelA*<sup>wt</sup> and *RelA*<sup>Δ</sup> pancreata. All acinar cells express  $\alpha$ -amylase independently of the genotype.  $\beta$ -actin was the loading control. (C) Images from pancreatic explants collected on days 0, 2, and 5 of culture with TGF $\alpha$  double-immunolabeled for  $\alpha$ -amylase (green) and CK19 (red). Scale bars, 50  $\mu$ m. (D) Quantification of duct-like structures from *RelA*<sup>wt</sup> (n=3) and *RelA*<sup>Δ</sup> (n=3) pancreatic explants formed following culture for 2 or 5 days with 50 ng/ml TGF $\alpha$ . Mean  $\pm$  SD; \*\*\*p<0.0001 by unpaired t test; n: number of mice. (E) Quantification of duct-like structures from *Kras* (n=2) and *Kras RelA* (n=2) pancreatic explants formed following culture for 5 days with 50 ng/ml TGF $\alpha$ . Mean  $\pm$  SD; \*\*\*p<0.0001 by unpaired t test; n: number of mice.



### Supplemental Figure 5. RelA deficiency compromises OIS

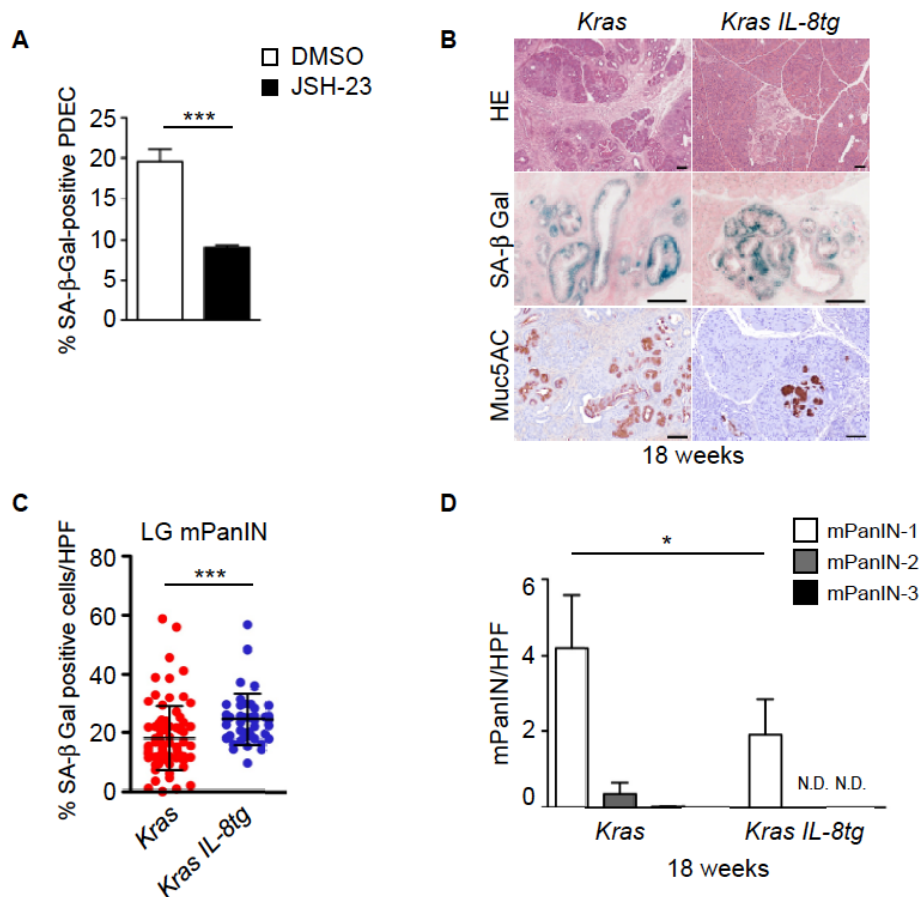
Quantification of immunoblot analysis of DCR2, p53, p16, p19 in lysates from *Kras* and *Kras RelA* mice, representing the pixel intensity. Mean  $\pm$  SD; \* $p < 0.05$  by unpaired t test.





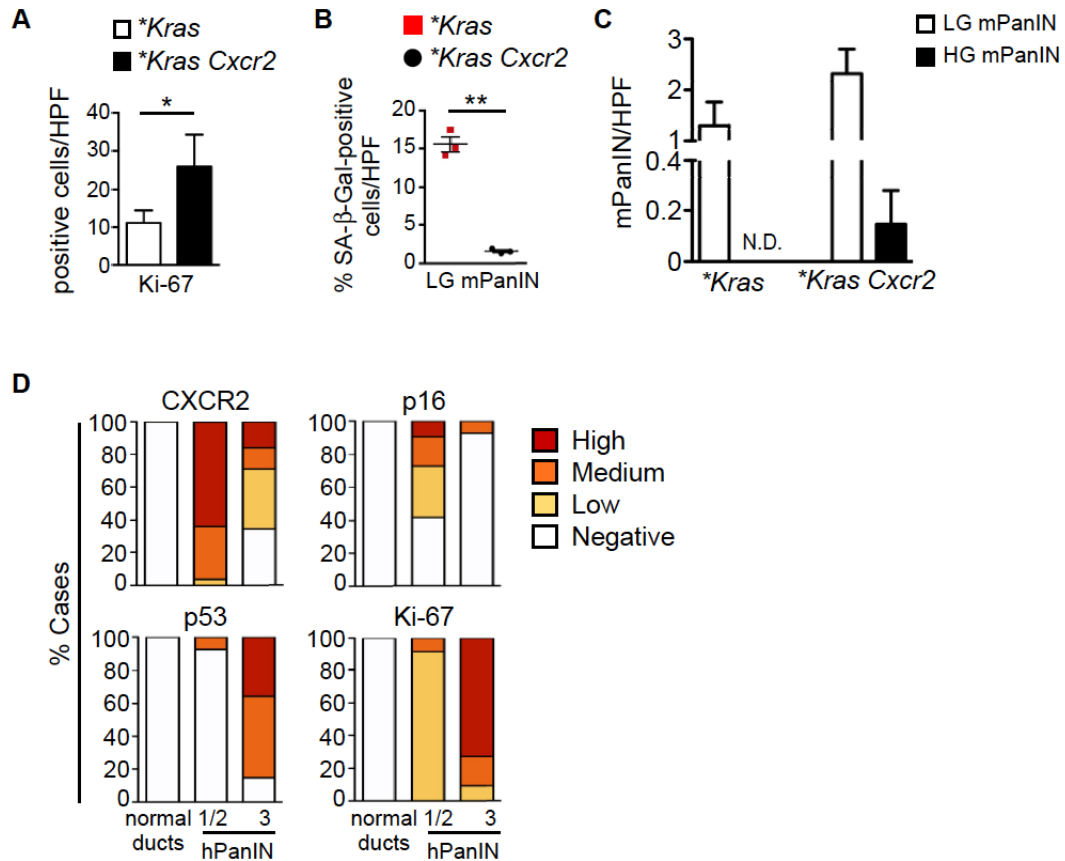
### Supplemental Figure 6. Characterization of immune response after pancreas-specific deletion of RelA in *Kras* mice

(A-F) Characterization of myeloid cells in pancreata from 8-week-old *Kras* (n=4) and *Kras RelA* (n=5) animals using flow cytometry analysis and immunohistochemistry. Data are presented as Mean ± SD; \*p<0.05, \*\*p<0.005 by Mann Whitney test; n: number of mice. Macrophages were sorted by FACS (CD11b<sup>+</sup>F4/80<sup>+</sup>) (A) and quantified (B) in *Kras* and *Kras RelA* mice. Pancreatic sections were stained with anti-F4/80 antibody; scale bars, 50µm (C). Quantitative analyses of CD11b<sup>+</sup>Gr-1<sup>+</sup> (D) and CD11b<sup>+</sup>Gr-1<sup>+</sup>CD206<sup>+</sup> (E) cells among CD45<sup>+</sup> positive cells. Pancreatic sections were stained with anti-CD206 antibody (F); black arrowheads indicate positive cells; scale bars, 50µm. (G) Real-time PCR expression analysis of indicated cytokines, chemokines, and *cox2* in pancreata from *Kras* (n=3) and *Kras RelA* (n=3) mice. Error bars are shown as standard deviations. Results are the average of three independent experiments and are presented as Mean ± SD; \*p<0.05, \*\*p<0.005 by unpaired t test; n: number of mice.



### Supplemental Figure 7. The regulation of senescence by RelA/p65 is mediated through CXCL1/KC

(A) Quantification of SA-β-Gal staining in *Kras* PDEC cultures treated with vehicle control (DMSO) or an NF-κB inhibitor (JSH-23). SA-β-Gal-positive cells were counted in 10 random high power fields (HPF). Mean ± SD; \*\*\* $p < 0.0005$  by unpaired t test. (B) Representative H&E staining, SA-β-Gal staining, and immunostaining for Muc5AC in low-grade mPanIN in pancreatic sections from 18-week-old *Kras* and *Kras IL-8tg* mice. Scale bars, 50 μm. (C) Ratio of SA-β-Gal positive mPanIN cells to the total number of mPanIN cells in low-grade mPanIN (LG mPanIN) in 18-week-old *Kras* (5 mice) and *Kras IL-8tg* (3 mice) was counted per 200x optical field (high power field, HPF). Mean ± SD;  $n \geq 44$ ; \*\*\* $p < 0.0005$  by Mann Whitney test; n: number of HPF. (D) Numbers of mPanINs in 18-week-old *Kras* ( $n=5$ ) and *Kras IL-8tg* ( $n=3$ ) mice were counted per 200x optical field (high power field, HPF). Mean ± SD; \* $p < 0.05$  by unpaired t test; N.D., not detectable; n: number of mice.



### Supplemental Figure 8. Evidence of SASP/CXCR2 axis in human PDAC

(A) Quantification of Ki-67 positivity 18-week-old *\*Kras* (n=3) and *\*Kras Cxcr2* (n=3) mice. Mean  $\pm$  SD; \*p<0.05, by unpaired t test; 200x optical field (high power field, HPF); n: number of mice. (B) Ratio of SA- $\beta$ -Gal positive mPanIN cells to the total number of mPanIN cells in low-grade mPanIN (LG mPanIN) in *\*Kras* (n=3) and *\*Kras Cxcr2* (n=3) mice. Mean  $\pm$  SEM; \*\*p<0.005, by unpaired t test; 200x optical field (high power field, HPF); n: number of mice. (C) Numbers of low-grade (LG) and high-grade (HG) mPanIN in 18-week-old *\*Kras* (n=2) and *\*Kras Cxcr2* (n=3) mice were counted per 200x optical field (high power field, HPF). Mean  $\pm$  SD; N.D., not detectable; n: number of mice. (D) Immunohistological examination and classification of the expression of CXCR2, p16, p53, and Ki-67 in human normal ducts, low- (hPanIN-1/2), and high-grade (hPanIN-3) hPanIN lesions. A total score of 0 was considered negative; a score of 1-2 - low; a score of 3-4 - medium; a score of 5-6 - high.

## Supplemental Methods

### Immunohistochemistry and immunofluorescence

Pancreata were removed, fixed overnight in 4% (wt/vol) buffered paraformaldehyde (Cat. No. 15710, Electron Microscopy Sciences, Hatfield, PA, USA) at 4°C, and embedded in paraffin. Paraffin sections (3.5 µm) were stained using standard immunohistochemical procedures. Signals were developed by the avidin-biotin peroxidase method using a 3,3'-diaminobenzidine substrate kit (Cat. No. SK-4100, Vector Laboratories, Peterborough, UK). The specificity of staining was confirmed for each antibody by control experiments, in which the primary antibody was omitted. Bright-field images were acquired on a Zeiss Axio1 imager with an AxioCam HRc camera (Zeiss, Oberkochen, Germany). To prepare cryosections, freshly isolated pancreatic tissue was embedded in Tissue-Tek® OCT™ compound (Sakura Finetek, Alphen aan Den Rijn, Netherlands), shock-frozen, sectioned at 7 µm thickness, and subjected to immunofluorescence staining.

### Proliferation

Mice were injected intraperitoneally with 50 mg/kg BrdU (Cat. No. B5002, Sigma Aldrich, Munich, Germany) 2 hr before sacrifice, and paraffin sections were stained with α-BrdU (Cat. No. RPN202, GE Healthcare, Munich, Germany). Representative pictures were taken at 200-fold magnification. BrdU-positive cells were counted in pancreatic sections from 3 to 5 animals of each genotype. The average number of positive cells and the standard deviations were calculated for all groups.

### Determination of cell number

To determine cell number and viability, cells were seeded into 6-well microplates at a concentration of  $5 \times 10^4$  cells/well and incubated at 37°C with 5% CO<sub>2</sub> in DMEM medium supplemented with 10% FCS, 5% non-essential amino acids, and 1X penicillin/streptomycin. After 24h, 48h, 72h, 96h, and 120 hours cells were harvested by trypsination. Subsequently, the cell suspension was supplemented with Guava ViaCount Reagent according to the manufacturer's protocol (Cat. No. 4000-0040). Viable cells were counted using the Guava® easyCyte 8HT Benchtop Flow Cytometer (Cat. No. 0500-4008), and analyzed with the InCyte™ and GuavaSuite Software (EMD Millipore, Billerica, MA, USA)

### Immunoblotting

Pancreatic tissue and cells were lysed, and blots were performed as described previously (3). Nuclear extracts from cancer cells were prepared using Qproteome Cell Compartment Kit per the manufacturer's recommendation (Cat. No. 37502, Qiagen, Hilden, Germany).

### Antibodies used for Immunohistochemistry and immunofluorescence, and Immunoblotting

The following antibodies were used for immunohistochemistry analyses: CK19 (Troma-III, Developmental Studies Hybridoma Bank, Iowa City, IA, USA), Muc5AC (45M1, Cat. No. MA5-12178, Thermo Fisher Scientific, Waltham, MA, USA), F4/80 (Cat. No. MF48000, Thermo Fisher Scientific), HIF-1β (H-85, Cat. No. sc-22840, Santa Cruz, Dallas, TX, USA), RelA/p65 (A, Cat. No. sc-109, Santa Cruz), p21 (C-19, Cat. No. sc-397, Santa Cruz), Sox9 (Cat. No. AB5535, EMD Millipore, Billerica, MA, USA), γH2AX (Anti-phospho-Histone H2A.X (Ser139), clone JBW301, Cat. No. 05-

636, EMD Millipore), Dcr2 (Cat. No. ADI-AAP-371-E, Enzo Life Sciences, Lörrach, Germany), p53 (NCL-p53-CM5p, Leica Biosystems, Newcastle, UK), p19 (Cat. No. ab80, Abcam, Cambridge, MA, USA), CXCR2 (Cat. No. ab14935, Abcam), Ki-67 (Cat. No. ab15580, Abcam), p-Stat3 (Cat. No. 9145, Cell Signaling, Danvers, MA, USA), p-Erk (Cat. No. 4376, Cell Signaling), p-I $\kappa$ B $\alpha$  ((Ser32/36) 5A5, Cat. No. 9246, Cell Signaling), p-c-Jun ((Ser73) (D47G9) XP $\text{\textcircled{R}}$ , Cat. No. 3270, Cell Signaling), CD206 (Cat. No. 18704-1-AP, Proteintech, Rosemont, IL, USA).

The following antibodies were used for immunofluorescence staining: RelA/p65 (A, Cat. No. sc-109, Santa Cruz),  $\alpha$ -Amylase (Cat. No. A8273, Sigma Aldrich, Munich, Germany), CK19 (Troma-III, Developmental Studies Hybridoma Bank).

The following antibodies were used for immunoblotting: RelA/p65 (C-20) (Cat. No. sc-372, Santa Cruz), I $\kappa$ B $\alpha$  (C-21, Cat. No. sc-371, Santa Cruz),  $\beta$ -actin (Cat. No. A5441, Sigma Aldrich), LaminA/C (H-110, Cat. No. sc-20681, Santa Cruz), Dcr2 (Cat. No. ADI-AAP-371-E, Enzo Life Sciences), p16 (F-156, Cat. No. sc-1207, Santa Cruz), p19 (Cat. No. ab80, Abcam), p53 (NCL-p53-CM5p, Leica Biosystems), CK8 (Cat. No. 61038, Progen Biotechnik, Heidelberg, Germany), CK18 (Cat. No. 61028, Progen Biotechnik),  $\alpha$ -amylase (Cat. No. A8273, Sigma Aldrich).

### **Ras activation assay**

Ras-GTP levels were measured using the Ras Activation Assay Kit per the manufacturer's instructions (Cat. No. 17-218, EMD Millipore, Billerica, MA, USA). Briefly, fresh pancreatic tissue was lysed in ice-cold MLB buffer (125 mM HEPES, pH 7.5, 750 mM NaCl, 5% Igepal CA-630, 50 mM MgCl<sub>2</sub>, 5 mM EDTA, and 10% glycerol). Equal amounts of protein were incubated with Raf-1 RBD agarose beads for 45 min at 4°C with gentle agitation. After centrifugation, the supernatant was discarded, and the beads were washed 3 times with MLB, re-suspended in Laemmli reducing sample buffer, and subjected to Western blot with anti-RAS (clone RAS 10).

### **RNA isolation**

Total RNA from fresh pancreatic tissue was extracted using the RNeasy Mini Kit (Cat. No. 74104, Qiagen, Hilden, Germany) and reverse-transcribed with SuperScript $\text{\textcircled{R}}$  II Reverse Transcriptase (Cat. No. 18064014, Thermo Fisher Scientific, Waltham, MA, USA). RT-PCR analysis was performed using *Power SYBR $\text{\textcircled{R}}$  Green PCR Master Mix* (Cat. No. 4368577, Thermo Fisher Scientific, Waltham, MA, USA). All samples were amplified in duplicate and normalized against cyclophilin as an internal control. Quantification was performed using the delta-delta CT method. Primer sequences are available on request.

### **Primers for Quantitative RT-PCR Analyses**

The sequences used for quantitative RT-PCR analysis were as follows:

m-DCR2 forward	5'-AGCTAACCCAGCCCATTAATCGTC-3'
m-DCR2 reverse	5'-AGTTCCTTCTGACAGGTAAGTGGC-3'
m-Dec1 forward	5'-GGCGGGGAATAAAACGGAGCGA-3'
m-Dec1 reverse	5'-CCTCACGGGCACAAGTCTGGAA-3'
m-p53 forward	5'-AGATCCGCGGGCGTAAAC-3'
m-p53 reverse	5'-TCTGTAGCATGGGCATCCTTT-3'
m-p21 forward	5'-CACAGCGATATCCAGACATTCAG-3'
m-p21 reverse	5'-CGGAACAGGTCCGACATCA-3'
m-TNF $\alpha$ forward	5'-ACGGCATGGATCTCAAAGAC-3'
m-TNF $\alpha$ reverse	5'-AGATAGCAAATCGGCTGACG-3'

m-IFN $\gamma$ forward	5'-CATGGCTGTTTCTGGCTGTTACTG-3'
m-IFN $\gamma$ reverse	5'-GTTGCTGATGGCCTGATTGCTTTT-3'
m-IL-23p19 forward	5'-AATAATGTGCCCCGTATCCAGT-3'
m-IL-23p19 reverse	5'-GCTCCCCTTTGAAGATGTCAG-3'
m-IL12b forward	5'-ATGGAGTCATAGGCTCTGGAAA-3'
m-IL12b reverse	5'-CCGGAGTAATTTGGTGCTTCAC-3'
m-Cox-2 forward	5'-GCTGCCCGACACCTTCAACATT-3'
m-Cox-2 reverse	5'-CACATTTCTTCCCCCAGCAACC-3'

### **Preparation and culture of pancreatic ductal epithelial cells (PDEC)**

Whole adult mouse pancreata were harvested and digested in 1.0 mg/mL collagenase type V (Cat. No. C9263, Sigma Aldrich, Munich, Germany) at 37°C for 20 min on a shaker. Following several washes with HBSS (Cat. No. 14175-053, Thermo Fisher Scientific, Waltham, MA, USA), supplemented with 0.9 g/L glucose (Cat. No. G7528, Sigma Aldrich, Munich, Germany), the collagenase-digested pancreatic tissue was filtered through a Corning® 100 $\mu$ m Cell Strainer (Cat. No. 431752, Corning, New York, USA). Ductal cells were purified by centrifugation through HBSS solution and re-suspended in DMEM/F12 medium (Cat. No. 41965-039, Thermo Fisher Scientific, Waltham, MA, USA), supplemented with 5 mg/ml D-glucose (Cat. No. G7528, Sigma Aldrich, Munich, Germany), 0.1 mg/ml soybean trypsin inhibitor type I (Cat. No. T9003, Sigma Aldrich, Munich, Germany), 5 ml Insulin-Transferrin-Selenium (Cat. No. 41400-045, Thermo Fisher Scientific, Waltham, MA, USA), 25  $\mu$ g/ml bovine pituitary extract (Cat. No. 13028014, Thermo Fisher Scientific, Waltham, MA, USA), 20 ng/ml epidermal growth factor (Cat. No. 354001, Corning, New York, USA), 5 nM 3,3',5-triiodo-L-thyronine (Cat. No. T2877, Sigma Aldrich, Munich, Germany), 1  $\mu$ M dexamethasone (Cat. No. D1756, Sigma Aldrich, Munich, Germany), 1.22 mg/ml nicotinamide (Cat. No. 72340, Sigma Aldrich, Munich, Germany), 5% Nu-serum IV (Cat. No. 355504, Corning, New York, USA) 100 ng/ml cholera toxin (Cat. No. C8052, Sigma Aldrich, Munich, Germany), and Penicillin-Streptomycin (10,000 U/mL) (Cat. No. 15140-122, Thermo Fisher Scientific, Waltham, MA, USA). Cells were divided for 2-D culture on plates pre-coated with Corning® Collagen I, Rat Tail (Cat. No. 354236, Corning, New York, USA). SB225002 (an antagonist of CXCR2, 10  $\mu$ M; Cat. No. 2725, TORCIS Bioscience, Bristol, UK), or CXCL1/KC (100 ng/ml; Cat. No. CHM-335, BioSupply, Bradford, UK), or JSH-23 (blocks nuclear translocation of p65 and its transcription activity, 10  $\mu$ M; Cat. No. 481408, Thermo Fisher Scientific, Waltham, MA, USA) were added to the cells. 0,001% DMSO (Cat. No. D5879, Sigma Aldrich, Munich, Germany) (vehicle) was added as a control.

### **Preparation and culture of pancreatic acinar epithelial explants**

Pancreatic acinar epithelial explants of adult pancreatic tissue (5 weeks) were isolated using a standard collagenase digestion method, as previously described (4). Acinar explants were cultured by modification of a previously published protocol (5). Briefly, pancreata of mice were injected with collagenase type VIII (Cat. No. C2139, Sigma Aldrich, Munich, Germany) and incubated at 37°C for 20 min with shaking. Collagenase-digested pancreatic tissue was filtered through a Corning® 100 $\mu$ m Cell Strainer (Cat. No. 431752, Corning, New York, USA). Acinar explants were purified by centrifugation through McCoy's Medium (Cat. No. M9309, Sigma Aldrich, Munich, Germany), containing 0.1% BSA. Acinar cell viability was assessed by the trypan blue exclusion method. More than 80% of isolated acini were intact. Acinar explants were incubated at 37°C in DMEM/F12 Medium (Cat. No. 11320033, Thermo Fisher

Scientific, Waltham, MA, USA) supplemented with 10% FBS for 1h at 37°C. Thereafter, cells were pelleted and re-suspended in culture medium Waymouht's MB 752/1 (Cat. No. W1625, Sigma Aldrich, Munich, Germany) supplemented with 0.2 mg/ml soybean trypsin Inhibitor (Cat. No. T9003, Sigma Aldrich, Munich, Germany); 50 µg/ml bovine pituitary extract (Cat. No. 13028014, Thermo Fisher Scientific, Waltham, MA, USA), Insulin-Transferrin-Selenium (Cat. No. 41400-045, Thermo Fisher Scientific, Waltham, MA, USA), Penicillin-Streptomycin (10,000 U/mL) (Cat. No. 15140122, Thermo Fisher Scientific, Waltham, MA, USA), and an equal volume of Corning® Collagen I, Rat Tail (Cat. No. 354236, Corning, New York, USA). The cellular/collagen suspension was immediately plated on plates pre-coated with 2.5 mg/ml of Corning® Collagen I, Rat Tail. After solidification of the collagen, culture medium was added. Explants were maintained in the presence or absence of recombinant human TGF $\alpha$  (Cat. No. 239-A, R&D Systems, Minneapolis, USA) (final concentration 50 ng/ml). Media were exchanged on days 1 and 3.

### **Senescence-associated $\beta$ -galactosidase staining**

Cryosections of mouse pancreata and PDECs were stained for senescence-associated  $\beta$ -galactosidase activity per the manufacturer's instructions (Cat. No. 9860, Cell Signaling Technology, Beverly, MA, USA). To assess color development, samples were examined on a Zeiss Axio1 imager with an AxioCam HRc camera (Zeiss, Oberkochen, Germany). To quantify SA- $\beta$ -Gal staining in pancreatic tissue, pancreatic ducts that contained at least 10%  $\beta$ -Gal-positive cells were scored as positive.

### **Mouse cytokine array**

Cytokine arrays were used to determine the relative levels of 40 different cytokines and chemokines. The array was performed by using the protocol provided by the manufacturer (Ary 006; R&D Systems, Abingdon, UK). After development, the films were scanned, and the images were quantified by using Image J.

### **Treatment with CXCR2 inhibitor SB225002**

Five-week-old *Kras* mice were injected intraperitoneally with 0.5 mg/kg SB225002 (Tocris Bioscience, Bristol, UK) or PBS as vehicle 2 times a week by modification of a previously published protocol (6). After 4 weeks of treatment, the mice were euthanized and dissected, and pancreatic tissue was processed for histological and immunohistochemical analyses.

### **Human pancreas samples**

Samples were obtained from patients with histologically confirmed pancreatic ductal adenocarcinoma (PDAC). Sections (3.5 mm) were cut from formalin-fixed paraffin-embedded samples for immunohistochemistry. The use of human tissue was approved by the local ethics committee, and samples were obtained after informed consent had been obtained. Immunohistochemical analyses for CXCR2, p53, Ki-67, p16, and IL-8 in human PanIN lesions were performed on formalin-fixed, paraffin-embedded tissue sections using the standard avidin-biotin peroxidase staining procedure. The intensity of the staining was scored from 0 - negative to 3 - high. The distribution of staining of the lesions (proportion score) ranged from 0 (0%) to 6 (100%). A total score of 0 was considered negative, a score of 1-2 was considered low, a score of 3-4 medium, and a score of 5-6 high.

### **Micro-dissection of human low-grade PanIN cells and tumor ductal cells**

For micro-dissection of cells from low-grade PanIN cells and tumor ductal cells, resected tumor specimens were kept on ice and subsequently snap-frozen and stored at -80°C. All patients gave informed consent according to the approval of the local ethics committee. For histological examination, frozen sections were routinely processed (thickness 5 µm, H&E staining) and normal ducts and cancer cells were identified. For isolation of normal ductal cells, medium-sized interlobular or large ducts were preferentially selected. Carcinomatous tissue, which contained no or only few inflammatory cells were preferentially evaluated in order to avoid bias during qPCR analysis due to the anticipated chemokine expression of immune cells. Tissue blocks containing the cells of interest were serially sectioned (10 µm sections). The slides were stained with hemalaun and immediately stored at -20°C. Areas with cells of interest were manually micro-dissected under a microscope (BH2, Olympus) using a sterile injection needle (size 0.65x25 mm). Micro-dissected cells were collected from 10-30 serial sections.

### **Comparison of chemokine expression of human low-grade PanIN cells and tumor ductal cells by quantitative real-time PCR**

RNA from micro-dissected cells was isolated with a PicoPure RNA isolation kit (Cat. No. KIT0204, Thermo Fisher Scientific, Waltham, MA, USA) following the manufacturer's instructions including a DNase I digestion. Total RNA concentration and RNA integrity were determined using an Agilent 2100 Bioanalyzer (Agilent Technologies, Oberhaching, Germany). Only high integrity RNA was used for further experiments. RNA was amplified with a MessageAmp™ II aRNA Amplification Kit (Cat. No. AM1751 Thermo Fisher Scientific, Waltham, MA, USA) according to the manufacturer's recommendations and reversely transcribed using a High Capacity cDNA Reverse Transcription kit (Cat. No. 4368814, Thermo Fisher Scientific, Waltham, MA, USA). cDNA was subjected to quantitative real-time PCR on TaqMan Low Density Arrays (Cat. No. 4362745, Thermo Fisher Scientific, Waltham, MA, USA) and differential expression of chemokines was calculated by the comparative CT-Method of gene expression.

### **MIA-PACA-2 Cell Line**

MIA-PACA-2 cell line (DSMZ No. ACC 733) was obtained from Leinniz-Institut DSMZ-Deutsche Sammlung von Mikroorganismen und Zellkulturen GmbH.

### **Microarray analysis of gene expression**

Total pancreatic RNA was prepared as described above. RNA was labeled and hybridized to mouse gene chip expression arrays (Affymetrix Mouse Genome 430A 1.0 Array) according to Affymetrix protocols. Gene chips were scanned and analyzed using Affymetrix Microarray Suite 5.0 (MAS 5.0).

GSEA v2.07 was provided by the Broad Institute of MIT and Harvard (<http://www.broad.mit.edu/gsea/>) (7). We used default parameters of the GSEA software package, except for permutation type ("genotype").

The SASP gene set comprised the 31 genes that were significantly up-regulated in senescent fibroblasts (8).

### **Statistics**

Differences between 2 groups were analyzed using GraphPad Prism 5 by unpaired t test or Mann-Whitney test as indicated in the figure legends. Data are displayed as



mean  $\pm$  standard deviation unless otherwise indicated. Kaplan-Meier curves were used to calculate the overall survival and statistically analyzed by a log rank test. A Fisher's exact test was used to evaluate the tumor incidence. For all statistical analyses, two-tailed P value,  $P < 0.05$  was considered statistically significant.

### **Study approval**

Animals were kept in conventional animal facilities. All animal experiments were performed according to the guidelines for the care and use of laboratory animals and were approved by the local ethics Committee (UK and Regierung Oberbayern).

## Supplemental References

1. Ling J, Kang Y, Zhao R, Xia Q, Lee DF, Chang Z, Li J, Peng B, Fleming JB, Wang H, et al. KrasG12D-induced IKK2/beta/NF-kappaB activation by IL-1alpha and p62 feedforward loops is required for development of pancreatic ductal adenocarcinoma. *Cancer Cell*. 2012;21(1):105-20.
2. Highfill SL, Cui Y, Giles AJ, Smith JP, Zhang H, Morse E, Kaplan RN, and Mackall CL. Disruption of CXCR2-mediated MDSC tumor trafficking enhances anti-PD1 efficacy. *Science translational medicine*. 2014;6(237):237ra67.
3. Lesina M, Kurkowski MU, Ludes K, Rose-John S, Treiber M, Kloppel G, Yoshimura A, Reindl W, Sipos B, Akira S, et al. Stat3/Socs3 activation by IL-6 transsignaling promotes progression of pancreatic intraepithelial neoplasia and development of pancreatic cancer. *Cancer Cell*. 2011;19(4):456-69.
4. Algül H, Wagner M, Lesina M, and Schmid RM. Overexpression of ErbB2 in the exocrine pancreas induces an inflammatory response but not increased proliferation. *International journal of cancer*. 2007;121(7):1410-6.
5. Wagner M, Weber CK, Bressau F, Greten FR, Stagge V, Ebert M, Leach SD, Adler G, and Schmid RM. Transgenic overexpression of amphiregulin induces a mitogenic response selectively in pancreatic duct cells. *Gastroenterology*. 2002;122(7):1898-912.
6. Ijichi H, Chytil A, Gorska AE, Aakre ME, Bierie B, Tada M, Mohri D, Miyabayashi K, Asaoka Y, Maeda S, et al. Inhibiting Cxcr2 disrupts tumor-stromal interactions and improves survival in a mouse model of pancreatic ductal adenocarcinoma. *The Journal of clinical investigation*. 2011;121(10):4106-17.
7. Subramanian A, Tamayo P, Mootha VK, Mukherjee S, Ebert BL, Gillette MA, Paulovich A, Pomeroy SL, Golub TR, Lander ES, et al. Gene set enrichment analysis: a knowledge-based approach for interpreting genome-wide expression profiles. *Proc Natl Acad Sci U S A*. 2005;102(43):15545-50.
8. Coppe JP, Patil CK, Rodier F, Krtolica A, Beausejour CM, Parrinello S, Hodgson JG, Chin K, Desprez PY, and Campisi J. A human-like senescence-associated secretory phenotype is conserved in mouse cells dependent on physiological oxygen. *PLoS One*. 2010;5(2):e9188.